Taylor & Francis
Taylor & Francis Group

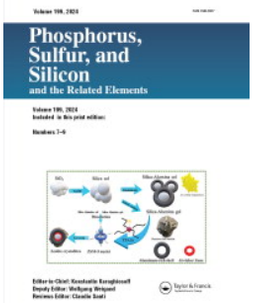

Phosphorus, Sulfur, and Silicon and the Related Elements

ISSN: 1042-6507 (Print) 1563-5325 (Online) Journal homepage: www.tandfonline.com/journals/gpss20

A novel process approach of a circular economy practice in the production of hydroxyapatite from phosphogypsum

Cemre Avşar & Suna Ertunç

To cite this article: Cemre Avşar & Suna Ertunç (2024) A novel process approach of a circular economy practice in the production of hydroxyapatite from phosphogypsum, Phosphorus, Sulfur, and Silicon and the Related Elements, 199:7-9, 628-634, DOI: 10.1080/10426507.2024.2410867

To link to this article: https://doi.org/10.1080/10426507.2024.2410867

PHOSPHORUS, SULFUR, AND SILICON AND THE RELATED ELEMENTS
2024, VOL. 199, NOS. 7–9, 628–634
https://doi.org/10.1080/10426507.2024.2410867

A novel process approach of a circular economy practice in the production of hydroxyapatite from phosphogypsum

Cemre Avşar[a,b] and Suna Ertunç[b]

[a]Research & Development Center, Toros Agri-Industry, Mersin, Turkey; [b]Department of Chemical Engineering, Ankara University, Ankara, Turkey

ABSTRACT

Phosphogypsum (PG), a by-product of phosphate fertilizer industry, is chemically impure gypsum ($CaSO_4 \cdot 2H_2O$) containing phosphate residues. Provided by the calcium and phosphorus content, PG can be considered as a precursor for synthetic hydroxyapatite (s-HAp) production. This study proposes a two-step alkali route for s-HAp production from PG. Resulting samples were characterized by ICP-OES, SEM, XRD and FT-IR analyses in comparison with bone ash (BA) sample. Ca/P ratio (wt%) was determined as 2.46 and 2.78 for s-HAp and BA samples, respectively. SEM analysis showed the uniform distribution of spherical shaped particles in BA samples; however s-HAp particles showed irregular distribution of nearly spherical-like particles agglomerated as platelets on the surface. XRD analysis indicated that s-HAp particles possessed low crystallinity and ICDD references showed the appearance of apatite-CaOH phases. FT-IR spectrum showed the vibration bands of PO_4^{3-} bands in the range of 1018–601 cm^{-1}. According to characterization analyses, s-HAp samples show lower Ca/P ratio, irregular morphology, and low crystallinity due to possible impurities. Thus, further downstream operations regarding to impurity removal should be employed to develop a promising route to synthetic HAp production and employ a CE approach on industrial scale to evaluate s-HAp samples as a commercial substitute to BA.

ARTICLE HISTORY
Received 21 August 2023
Accepted 24 August 2024

KEYWORDS
Calcium phosphate; hydroxyapatite; hydrothermal synthesis; phosphogypsum

GRAPHICAL ABSTRACT

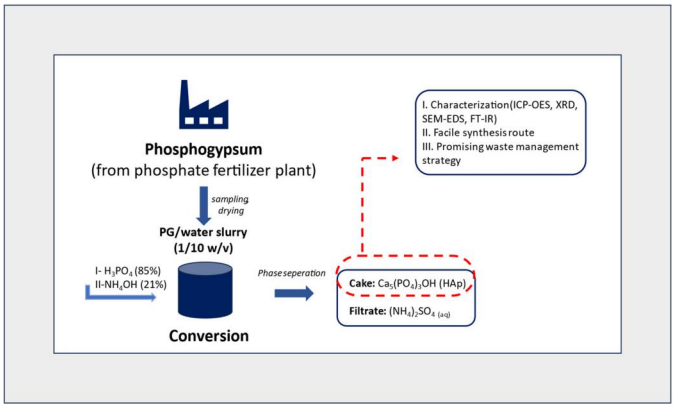

1. Introduction

Energy demand is the main priority of the ever-increasing global industrialization capacity. However, current technologies are intensively dependent on nonrenewable energy resources, resulting in irrepressible solid waste accumulation and climate change related to industry-based emissions. Circular Economy (CE) strategy is an effective driving force to all industrial sectors for implementing carbon emission reduction technologies to achieve 45% reduction target until 2030 and further achieve carbon neutrality until 2050.[1,2] Recent research hot spots are mostly related to greenhouse gas (GHG) emission reduction, environmental pollution, irreversible resource depletion and optimization in waste management strategies.[3–5]

Urgent demand to a better resource efficiency and focus to European Union Horizon 2020 strategy has let the term CE gain increasing attention during the past years among environmental researchers, economists, and industry.[6,7] CE strategy allows boosting resource efficiency *via* a transition to cleaner technologies, reduced pollution, and preserving biodiversity. One general definition of CE is maintaining product values, materials, and resources by introducing them to production cycle not for a single time and try to keep them in the loop as long as they are efficient, thus minimizing waste generation.[8,9]

From waste management point of view, CE can be defined as an approach for an effective waste management within the concept of the 3Rs, namely reduce, reuse, and

CONTACT Cemre Avşar cemre.avsar@toros.com.tr Research & Development Center, Toros Agri-Industry, 33020, Mersin, Turkey.

recycle.[10] From industrial point of view, industrially derived materials should be recovered through industrial recycling mechanisms to apply to the CE strategy. This study proposes preliminary studies for developing a novel approach for an industrially applicable CE model, in which phosphogypsum (PG) is converted into synthetic hydroxyapatite (s-HAp) particles, which have a high potential to be utilized as an alternative material to bone ash (BA) because of their structural similarity in terms of calcium and phosphorus content.

Current phosphate fertilizer production technologies rely on prior phosphoric acid production *via* wet process, basically defined as the reaction between phosphate rock and sulfuric acid. Reaction stoichiometry allows the generation of a by-product, PG.[11–13] PG is chemically gypsum in dihydrate form; however, it's purity is affected by process residues and phosphate rock-based impurities utilized in the wet process.[14–18] Approximately 4.5–5 tons of PG is generated per 1 ton phosphoric acid in the wet process, resulting annualy in generation of 200–350 Mtons of PG.[19] Conventional PG treatment strategies have been storage as piles near coastal regions or discharge into the sea, and these management procedures have hindered the evaluation potential of PG as a secondary raw material. However, emerging CE strategies have been supporting the development of more sustainable management and use strategies in the case of PG.

Mass generation amount and chemical structure as an impure gypsum attracts PG to be evaluated as secondary resources in the production cycles. Having Ca in form of CaO and P in form of P_2O_5 with 30–35 wt% and 0.9–1.8 wt%, respectively, PG can be an efficient precursor for synthetic hydroxyapatite particles. Phosphorus content in PG is relatively low, however the annual generation rate of PG would make it possible to provide a continuous phosphorus source in the production processes.[20–22]

Bone china is a specialty tableware product, having some advantages rather than delicate porcelain such as its whiteness, translucency, high glaze, and smoothness.[23,24] In addition, high mechanical strength makes bone china an attractive and expensive tableware product.[25] Although raw material selection and their composition differ, a typical bone china formulation has 50 wt% bone ash and 25 wt% clay. Rest 25 wt% can be a fluxing material such as Cornish stone or feldspar.[26–28] However, CE strategy from waste management point of view can be applied in such formulations, such as introducing industrial soda-lime silica glass waste in bone china composition, providing an applicable example to CE model on industrial scale.[29,30]

Synthetic HAp particles have very similar characteristics to natural bone ash, namely natural HAp, on chemical and crystallographic basis.[19] Although decomposition of bone ash to β-tricalcium phosphate, lime, and water starts at temperatures higher than 775 °C, the dominant structure in natural bone ash is HAp after calcination at 1000 °C.[27,28] In this manner, synthetic PG-derived HAp particles can also be a substitute to natural bone ash in the bone china composition for commercial applications. This route would provide an effective waste valorization strategy and an industrially applicable CE model. Although there are various studies discussing bone ash material for bone china production, studies regarding to the evaluation of synthetic HAp particles are limited.[31] The novelty of this study is the production of PG-derived s-HAp particles and the evaluation for bone china production as a substitute to BA, which has not been previously discussed.

2. Results and discussion

Owing to approx. 30–35 wt% CaO content in its structure, PG plays a role as the Ca source in s-HAp particles. Relatively low P_2O_5 content (approx. 1 wt%) in PG's structure might be stoichiometrically inadequate, however H_3PO_4 addition in the reaction media acts as the phosphorus source in the proposed process. Table 1 gives the Ca/P ratio of s-HAp sample together with BA sample obtained by ICP-OES analysis. Ca/P ratio, indicating the structural similarity of synthetic and natural HAp particles, is an important characteristic for industrial applicability of s-HAp particles.

The ideal molar Ca/P ratio of HAp particles is 1.67. According to the molar ratio, the mass ratio can be computed as 2.16. Synthetic HAp particles produced for commercial applications have a Ca/P ratio of 3–3.2 by mass and those synthesized through hydrothermal routes have a Ca/P ratio of 1.86–2.08.[32,33] Table 1 shows that even though the ICP-OES analysis results were consistent with previous literature, the presence of PG based impurities in s-HAp particles resulted in a Ca/P ratio greater than the stoichiometric ratio.

Figure 1 gives the XRD analysis results of s-HAP and BA samples in comparison to ICDD file 98-015-1414 as the reference. According to XRD data, peaks observed at 2θ 25.42° and 25.44° denotes for the quartz phases in s-HAp and BA samples, respectively. High intensity quartz peak obtained in s-HAp sample indicates the low conversion ratio of PG to HAp. Peaks observed at 2θ 30.93° and 29.61° are attributed to tricalcium phosphate phases in s-HAp and BA samples, respectively.[34,35] β-TCP phases are more distinct and narrower in the spectrum of the BA sample, and better crystallinity was obtained from the partial breakdown of BA sample into β-TCP phase. Pure and uniform structure in BA sample was indicated by higher intensity-peaks compared to s-HAp sample. Relatively low-intensity peaks attributed to β-TCP phase in s-HAp sample indicated possible PG-based contaminants affecting the purity of the sample. According to XRD analysis, calcination at higher temperatures might improve the degree of crystallinity of the s-HAp samples.[26,27]

Figure 2 gives the SEM images of the samples, indicating that both samples possess individual morphological characteristics. BA samples (Figure 2(b)) showed uniform distribution of spherical-shape nanoparticles with an average size of 2–3 nm. However, s-HAp sample (Figure 2(a)) showed

Table 1. Ca/P ratio of s-HAp and BA samples.

wt%	CaO	Ca	P	Ca/P
s-HAp	40.63	29.04	11.8	2.46
BA	42.30	30.23	10.8	2.79

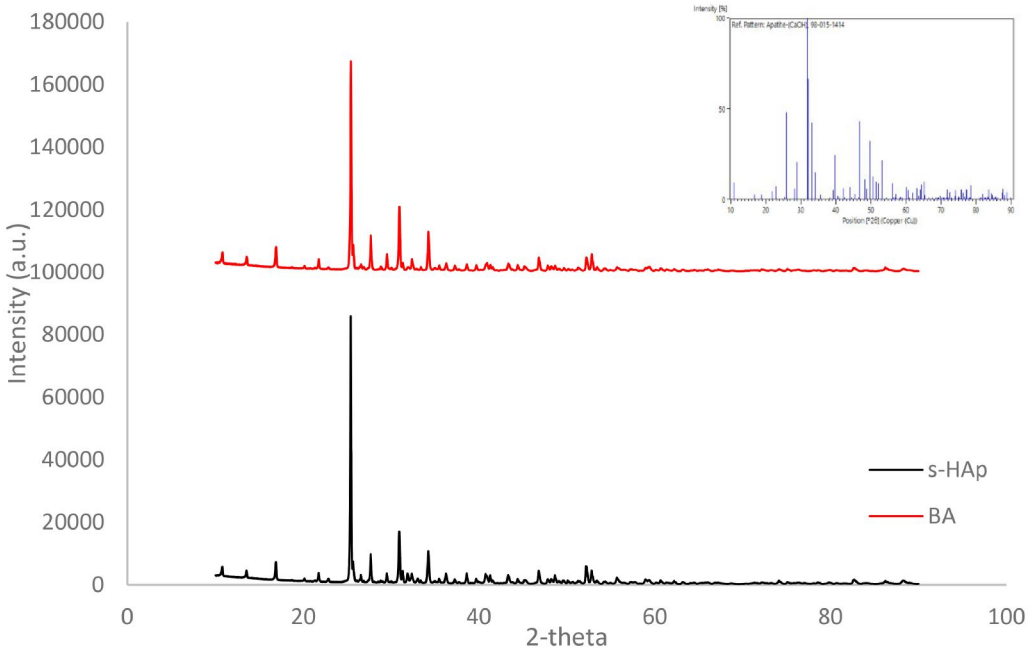

Figure 1. XRD analysis of s-HAp and BA samples.

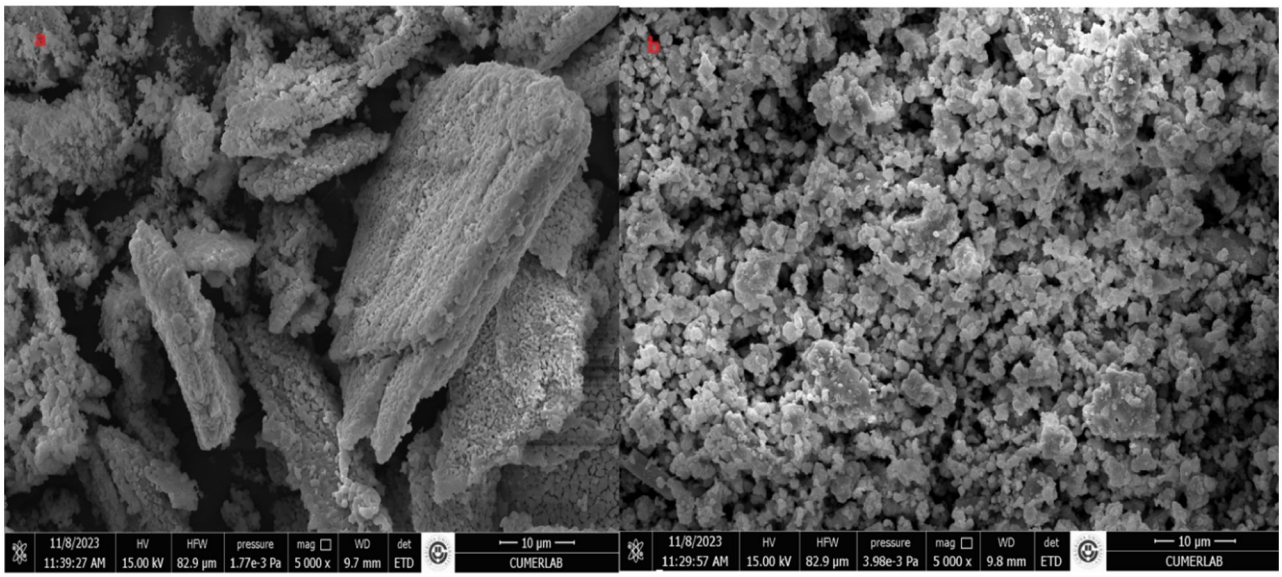

Figure 2. SEM images of s-HAp (a) and BA (b) samples.

irregularly distributed spherical like particles with approx. 0.5–1 nm particle size agglomerated as plate-like structures on the surface. Morphological characterization indicated that downstream operations such as purification should be needed for s-HAp particles.

Results obtained from FT-IR analysis performed on s-HAp particles are given in Figure 3.

Strong stretching vibration bands belonging to PO_4^{3-} groups are observed in the range of 1020–610 cm^{-1}, and a weak stretching vibration band belonging to PO_4^{3-} groups is observed in the range of 450 and 480 cm^{-1}. The stretching vibration bands at 1395 and 1400 cm^{-1} belong to the CO_3^{2-} groups in the s-HAp structure. It is assumed that the weak absorption bands at 838 and 870 cm^{-1} may belong to CO_3^{2-} groups. The OH bands observed in the spectrum at 1618, 1691, 3405 and 3539 cm^{-1} indicate that there is absorbed water in the sample structure and the s-HAp samples were not dried efficiently. In the literature regarding the relevant functional groups, data are reported for OH^- at 3573 cm^{-1}, bound water at 1641 cm^{-1}, CO_3^{2-} group at 1456 and 862 cm^{-1} and for PO_4^{3-} group at 1011, 567 and 473 cm^{-1}. The observed bands and the results are compatible with the literature.[34] The presence of CO_3^{2-} groups revealed a possible presence of carbonated hydroxyapatite (c-HAp) structure, however detailed characterization is required.[36,37]

ICP-OES analysis results revealed that Ca/P ratio of s-HAp and BA samples were comparable. However, XRD analysis showed that s-HAp particles display lower crystallinity than BA sample according to low intensity β-TCP phase peaks. SEM images showed the morphological differences

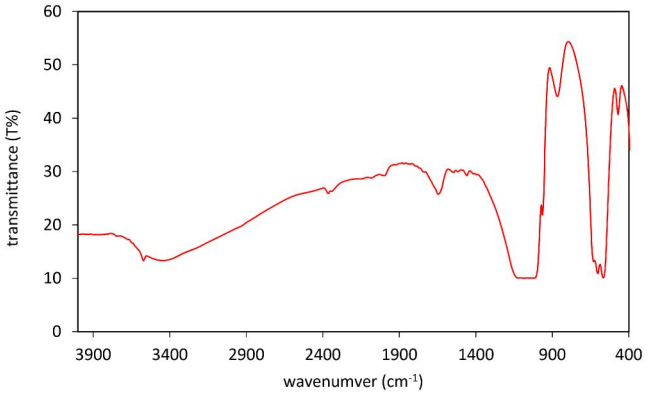

Figure 3. FT-IR spectrum of s-HAp sample.

between samples, indicating the irregular distribution of spherical-shape particles agglomerated as plates on s-HAp sample. BA samples showed homogenous distribution of spherical shape particles throughout the surface. The presence of characteristic functional groups in accordance with previous literature were verified by FT-IR analysis.

Previous literature lacks the comparison of BA sample with s-HAp particles. However, similar Ca/P ratio in s-HAp particles make them an appropriate candidate for BA material. When compared, vast amount of natural BA with complex and costly synthesis procedures of s-HAp particles might not be economically feasible currently. However, developing a synthesis route for s-HAp particles produced *via* PG conversion might pursue an effective waste management strategy. Economic feasibility studies should be required to open up a cost-effective route for the synthesis of s-HAp particles, further improvements in the synthesis route and post-purification studies might result to obtain s-HAp particles compatible to BA samples in industrial applications. Evaluating these s-HAp particles for bone china production as a substitute to bone ash would make PG a valuable commodity product and support CE applications on industrial scale.

3. Experimental

3.1. Materials and methods

PG can be evaluated for synthetic HAp production through various synthesis routes proposed in the literature. Although synthesis agents show differences according to the process employed, overall description can be stated as PG dissolution by mineral acids and further pH shift to alkaline media. Downstream operations include filtering, drying and calcination of the resulting HAp particles.[34,38–40] In this study, a hydrothermal method similar to those previously proposed by Mousa and Hanna was employed.[34] Thermodynamic evaluation of the reaction sequence was conducted to check the thermodynamic nature of the proposed synthesis route. s-HAp and BA samples were digested by microwave assisted temperature-controlled acid digestion method (Anton Paar Multiwave PRO) prior to ICP-OES analysis (Agilent Technologies 5110) to evaluate their Ca/P ratio. Morphology and crystallinity of resulting s-HAp sample was investigated by SEM (FEI Quanta 650) and XRD (Bruker D8 Venture) analyses, respectively. FT-IR (Shimadzu 8400) analysis was also performed to investigate the functional groups in the sample.

Table 2. Standard ΔH_f of reactants and products at 298.15 °C.

Reactants	ΔH_f (kJ/mol)	Products	ΔH_f (kJ/mol)
Gypsum	−1434.5	$Ca_5(PO_4)_3OH$	−4120.8
H_3PO_4	−1271.7	H_2O	−285.8
NH_4OH	−361.2	$(NH_4)_2SO_4$	−1180.9
H_2SO_4	−814		

3.2. Thermodynamic analysis of the proposed reaction sequence

Equations (1) and (2) gives the two-step reaction sequence proposed in this study similar to those proposed by Mousa and Hanna.[34]

$$5\ CaSO_4 \cdot 2\ H_2O + 3\ H_3PO_4 \rightarrow Ca_5(PO_4)_3OH + 5\ H_2SO_4 + 19\ H_2O \quad (1)$$

$$10\ NH_4OH + 5\ H_2SO_4 \rightarrow 5(NH_4)_2SO_4 + 10\ H_2O \quad (2)$$

From Equations (1) and (2), the overall reaction can be given as Equation (3) below:

$$5\ CaSO_4 \cdot\ 2\ H_2O + 3\ H_3PO_4 + 10\ NH_4OH \rightarrow Ca_5(PO_4)_3OH + 5(NH_4)_2SO_4 + 19\ H_2O \quad (3)$$

The thermodynamic analysis of Equation (3) was carried out prior to carrying out the reaction sets in order to determine whether the suggested reaction is thermodynamically possible. Table 2 provides the standard enthalpy of formation (ΔH_f (kJ/mol)) of reactants and products of Equations (1) and (2) at 298.15 °C.[41]

According to the data given in Table 1, ΔH_f values of reactions (1) and (2) are calculated as −2633.4 and −1080.5 kJ/mol, respectively. Since both reactions are exothermic, it can be said that the reaction sequence is thermodynamically spontaneous under experimental conditions and increase in temperature would reduce equilibrium constant (K) and adversely affect the product concentration at equilibrium. Thus, reaction sets were performed under ambient pressure and temperature (25 °C).

3.3. Experimental procedure

Figure 4 gives a schematic illustration of the experimental procedure.

PG was sampled from the stockpile of a fertilizer producer located in southern Turkey and dried until constant mass, further sieved below 125 µm particle size to obtain uniform particle size distribution. Slurry of PG/water with 1/10 solid/liquid ratio was prepared and put into the reactor; stoichiometric amount of analytical grade H_3PO_4 (85%) was used as the degradation agent in reaction media. Solid/liquid ratio was prepared as 1/10 (s/l) to overcome the diffusion resistance in the solid/liquid interface during reaction.

Figure 4. Schematic illustration of the experimental process.

NH_4OH (21%) was fed to the reactor to shift the pH to alkali region (approx. 9–10). Once the pH shifts to alkali conditions, Ca-P particles begin to precipitate and ammonium sulfate (AS) forms in aqueous phase. Reaction was terminated after 3 h, solid and liquid phases were separated by filtration and the obtained solid phase (s-HAp and unconverted PG) were dried at 80 °C in oven (Thermo Scientific MaxQ 6000) overnight.

4. Conclusions

Comparison of synthetic HAp particles with natural bone ash has not been discussed in detail in previous literature. Costly and troublesome synthesis routes of synthetic HAp make the material economically unfeasible to be a commercial substitute to bone ash. This study proposed a facile hydrothermal method composed of a two-step heterogenous reaction set to produce s-HAp particles from PG. ICP-OES analysis revealed the Ca/P ratio of s-HAp and BA samples as 2.46 and 2.78 by mass, respectively. XRD analysis indicated low intensity β-TCP phases in s-HAp particles and distinct quartz peaks, suggesting low crystalline structure and low conversion ratio of PG. SEM images also showed the morphological differences between the two samples, s-HAp showing randomly distributed platelets composing of spherical-shape agglomerates. BA sample showed homogenous distribution of spherical nanoparticles throughout the surface. FT-IR spectrum showed the characteristic bonds of phosphate groups, however the presence of carbonate groups revealed possible impurities in the form of c-HAp particles. Characterization studies show that HAp particles can be produced through the proposed hydrothermal synthesis route, however further detailed reaction optimization studies are required to optimize the sequence in economically feasible manner. This study might be a guide to develop a synthesis route to produce s-HAp particles from PG, which is abundant and needs to be evaluated. Further studies regarding the development of the synthesis route proposed in this study might provide the commercial application of PG-based s-HAp particles as a substitute to bone ash in bone china production. However, more research is necessary to determine whether utilizing as a tableware product might pose health problems due to PG based impurities, in this manner effective purification operations might be important to reduce health risks.

Open Scholarship

This article has earned the Center for Open Science badge for Open Materials. The materials are openly accessible at re3data.org.

Disclosure statement

No potential conflict of interest was reported by the author(s).

Funding

This study is financially supported by The Scientific and Technological Research Council of Turkey [TÜBİTAK, Project No: 118C085] and conducted between the co-operation of Ankara University and Toros AGRI Industry and Trade Co. Inc. R&D Center within the scope of TÜBİTAK 2244 Industrial PhD Fellowship Program.

ORCID

Cemre Avşar http://orcid.org/0000-0002-8953-9859
Suna Ertunç http://orcid.org/0000-0002-0139-7463

References

[1] Yang, M.; Chen, L.; Wang, J.; Msigwa, G.; Osman, A. I.; Fawzy, S.; Rooney, D. W.; Yap, P. S. Circular Economy Strategies for Combating Climate Change and Other Environmental Issues. *Environ. Chem. Lett.* **2023**, *21*, 55–80. DOI: 10.1007/s10311-022-01499-6.

[2] Wang, P.; Yang, Y. Y.; Heidrich, O.; Chen, L. Y.; Chen, L. H.; Fishman, T.; Chen, W. Q. Regional Rare-Earth Element Supply and Demand Balanced with Circular Economy Strategies. *Nat. Geosci.* **2024**, *17*, 94–102. DOI: 10.1038/s41561-023-01350-9.

[3] Zhang, A.; Venkatesh, V. G.; Liu, Y.; Wan, M.; Qu, T.; Huisingh, D. Barriers to Smart Waste Management for a Circular Economy in China. *J. Clean. Prod.* **2019**, *240*, 118198. DOI: 10.1016/j.jclepro.2019.118198.

[4] Sadhukhan, J.; Dugmore, T. I. J.; Matharu, A.; Martinez-Hernandez, E.; Aburto, J.; Rahman, P. K. S. M.; Lynch, J. Perspectives on "Game Changer" Global Challenges for Sustainable 21st Century: Plant-Based Diet, Unavoidable Food Waste Biorefining, and Circular Economy. *Sustainability* **2020**, *12*, 1976. DOI: 10.3390/su12051976.

[5] Dantas, T. E. T.; de-Souza, E. D.; Destro, I. R.; Hammes, G.; Rodriguez, C. M. T.; Soares, S. R. How the Combination of Circular Economy and Industry 4.0 Can Contribute Towards Achieving the Sustainable Development Goals. *Sustain. Prod. Consum.* **2021**, *26*, 213–227. DOI: 10.1016/j.spc.2020.10.005.

[6] Geisendorf, S.; Pietrulla, F. The Circular Economy and Circular Economic Concepts- a Literature Analysis and Redefinition. *Thunderbird Int. Bus. Rev.* **2017**, *60*, 771–782. DOI: 10.1002/tie.21924.

[7] Halkos, G. E.; Aslanidis, P.-S. C. How Waste Crisis Altered the Common Understanding: From Fordism to Circular Economy and Sustainable Development. *CircEconSust.* **2024**, *4*, 1513–1537. DOI: 10.1007/s43615-023-00337-3.

[8] Martínez-Martínez, S.; Pérez-Villarejo, L.; Eliche-Quesada, D.; Sánchez-Soto, P. J. New Types and Dosages for the Manufacture of Low-Energy Cements from Raw Materials and Industrial Waste under the Principles of the Circular Economy and Low-Carbon Economy. *Materials (Basel)* **2023**, *16*, 802. DOI: 10.3390/ma16020802.

[9] Herrador, M.; Van, M. L. Circular Economy Strategies in the ASEAN Region: A Comparative Study. *Sci. Total Environ.* **2024**, *908*, 168280. DOI: 10.1016/j.scitotenv.2023.168280.

[10] Ghisellini, P.; Cialani, C.; Ulgiati, S. A Review on Circular Economy: The Expected Transition to a Balanced Interplay of Environmental and Economic Systems. *J. Clean. Prod.* **2016**, *114*, 11–32. DOI: 10.1016/j.jclepro.2015.09.007.

[11] Bouargane, B.; Laaboubi, K.; Biyoune, M. G.; Bakiz, B.; Atbir, A. Effective and Innovative Procedures to Use Phosphogypsum Waste in Different Application Domains: Review of the Environmental, Economic Challenges and Life Cycle Assessment. *J. Mater. Cycles Waste Manag.* **2023**, *25*, 1288–1308. DOI: 10.1007/s10163-023-01617-8.

[12] Wang, Y.; Huo, H.; Chen, B.; Cui, Q. Development and Optimization of Phosphogypsum-Based Geopolymer Cement. *Constr. Build. Mater.* **2023**, *369*, 130577. DOI: 10.1016/j.conbuildmat.2023.130577.

[13] Mohammad, I.; Rana, A. S. Incorporation of Phosphogypsum with Cement in Rigid Pavement: An Approach Towards Sustainable Development. *Mater. Today: Proc., In Press*, **2023**. DOI: 10.1016/j.matpr.2023.03.586.

[14] Chernysh, Y.; Yakhnenko, O.; Chubur, V.; Roubík, H. Phosphogypsum Recycling: A Review of Environmental Issues, Current Trends, and Prospects. *Appl. Sci.* **2021**, *11*, 1575. DOI: 10.3390/app11041575.

[15] Silva, L. F. O.; Oliveira, M. L. S.; Crissien, T. J.; Santosh, M.; Bolivar, J.; Shao, L.; Dotto, G. L.; Gasparotto, J.; Schindler, M. A. Review on the Environmental Impact of Phosphogypsum and Potential Health Impacts Through the Release of Nanoparticles. *Chemosphere* **2022**, *286*, 131513. DOI: 10.1016/j.chemosphere.2021.131513.

[16] Ben Moussa, K.; Eturki, S.; Van Poucke, R.; Bodé, S.; De Grave, J.; Van Ranst, E.; Tack, F. M. G.; Moussa, M. Evaluating the Adsorptive Capacity of Three Tunisian Clays Deposits for Several Potentially Toxic Metals in Phosphogypsum Waste. *Arab. J. Geosci.* **2022**, *15*, 911. DOI: 10.1007/s12517-022-10073-x.

[17] Guan, Q.; Wang, Z.; Zhou, F.; Yu, W.; Yin, Z.; Zhang, Z.; Chi, R.; Zhou, J. The Impurity Removal and Comprehensive Utilization of Phosphogypsum: A Review. *Materials (Basel)* **2024**, *17*, 2067. DOI: 10.3390/ma17092067.

[18] Ennaciri, Y.; Bettach, M. The Chemical Behavior of the Different Impurities Present in Phosphogypsum: A Review. *Phosphorus, Sulfur. Silicon Relat. Elem.* **2024**, *199*, 129–148. DOI: 10.1080/10426507.2023.2281489.

[19] Avşar, C.; Gezerman, A. O. An Evaluation of Phopshogypsum (PG)-Derived Nanohydroxyapatite (HAP) Synthesis Methods and Waste Management as a Phosphorus Source in the Agricultural Industry. *MS.* **2023**, *29*, 247–254. DOI: 10.5755/j02.ms.31695.

[20] Wang, J.; Dong, F.; Wang, Z.; Yang, F.; Du, M.; Fu, K.; Wang, Z. A Novel Method for Purification of Phoshogypsum. *Physicochem. Probl. Miner. Process.* **2020**, *56*, 975–983. DOI: 10.37190/ppmp/127854.

[21] Calderón-Morales, B. R. S.; García-Martínez, A.; Pineda, P.; García-Tenório, R. Valorization of Phosphogypsum in Cement-Based Materials: Limits and Potential in Eco-Efficient Construction. *J. Build. Eng.* **2021**, *44*, 102506. DOI: 10.1016/j.jobe.2021.102506.

[22] Cao, W.; Yi, W.; Peng, J.; Li, J.; Yin, S. Recycling of Phosphogypsum to Prepare Gypsum Plaster: Effect of Calcination Temperature. *J. Build. Eng.* **2022**, *45*, 103511. DOI: 10.1016/j.jobe.2021.103511.

[23] Zhang, Y.; Zhou, N.; Li, W.; Li, J.; Nian, S.; Li, X.; Sui, J. Fabrication and Characterization of Bone China Using Synthetic Bone Powder as Raw Materials. *Ceram. Int.* **2016**, *42*, 14910–14917. DOI: 10.1016/j.ceramint.2016.06.131.

[24] Kara, A.; Stevens, R. Characterization of Biscuit Fired Bone China Body Microstructure. Part I: XRD and SEM of Crystalline Phases. *J. Eur. Ceram. Soc.* **2002**, *22*, 731–736. DOI: 10.1016/S0955-2219(01)00371-5.

[25] Capoglu, A. Elimination of Discolouration in Reformulated Bone China Bodies. *J. Eur. Ceram. Soc.* **2005**, *25*, 3157–3164. DOI: 10.1016/j.jeurceramsoc.2004.07.008.

[26] Iqbal, Y.; Messer, P. F.; Lee, W. E. Microstructural Evolution in Bone China. *Br. Ceram. Trans.* **2000**, *99*, 193–199. DOI: 10.1179/096797800680938.

[27] Iqbal, Y.; Messer, Y.; Lee, W. E. Non-Equilibrium Microstructure of Bone China. *Br. Ceram. Trans.* **2000**, *99*, 110–116. DOI: 10.1179/096797800680811.

[28] Batista, S. A. F.; Messer, P. F.; Hand, R. J. Fracture Toughness of Bone China and Hard Porcelain. *Br. Ceram. Trans.* **2001**, *100*, 256–259. DOI: 10.1179/bct.2001.100.6.256.

[29] Carus, L. A.; Bragança, S. R. Bone China Formulated with Waste Glass. *Adv. Appl. Ceram.* **2013**, *112*, 169–175. DOI: 10.1179/1743676112Y.0000000065.

[30] Yeşilay, S. Production of Stoneware Clay Bodies by Using Industrial Soda-Lime-Silica Glass Waste. *J. Aust. Ceram. Soc.* **2019**, *55*, 747–758. DOI: 10.1007/s41779-018-0286-0.

[31] Mostari, S.; Zaman, T.; Rahman, S. Synthesis and Characterization of Bone & Teeth Ash and Analysis of Their Influence on the Properties of Bone China. *Int. J. Mater. Sci. Appl.* **2017**, *6*, 171–177. DOI: 10.11648/j.ijmsa.20170604.12.

[32] Giraldo-Betancur, A. L.; Espinosa-Arbelaez, D. G.; Real-López, A. D.; Millan-Malo, B. M.; Rivera-Muñoz, E. M.; Gutierrez-Cortez, E.; Pineda-Gomez, P.; Jimenez-Sandoval, S.; Rodriguez-García, M. E. Comparison of Physicochemical Properties of Bio and Commercial Hydroxyapatite. *Curr. Appl. Phys.* **2013**, *13*, 1383–1390. DOI: 10.1016/j.cap.2013.04.019.

[33] Mohd Pu'ad, N. A. S.; Abdul Haq, R. H.; Mohd Noh, H.; Abdullah, H. Z.; Idris, M. I.; Lee, T. C. Synthesis Method of Hydroxyapatite: A Review. *Mater. Today: Proc.* **2020**, *29*, 233–239. DOI: 10.1016/j.matpr.2020.05.536.

[34] Mousa, S.; Hanna, A. Synthesis of Nano-Crystalline Hydroxyapatite and Ammonium Sulfate from Phosphogypsum Waste. *Mater. Res. Bull.* **2013**, *48*, 823–828. DOI: 10.1016/j.materresbull.2012.11.067.

[35] Ślósarczyk, A.; Paszkiewicz, Z.; Paluszkiewicz, C. FTIR and XRD Evaluation of Carbonated Hydroxyapatite Powders Synthesized by Wet Methods. *J. Mol. Struct.* **2005**, *744-747*, 657–661. DOI: 10.1016/j.molstruc.2004.11.078.

[36] Elmourabit, M.; Zarki, Y.; Arfoy, B.; Allaoui, I.; Aghzzaf, A. A.; Raissouni, I.; Bouchta, D.; Chaouket, F.; Draoui, K. Phosphate Sludge Valorization as New Alternative Precursor for Carbonated Hydroxyapatite Nanostructures: Synthesis and

Characterization. *J. Mater. Cycles Waste Manag.* **2023**, *26*, 602–619. DOI: 10.1007/s10163-023-01863-w.

[37] Alif, M. F.; Arief, S.; Yusuf, Y.; Yunita, Y.; Ramadhani, J.; Triandini, S. Synthesis of Hydroxyapatite from *Faunus Ater* Shell Biowaste. *Next Mater.* **2024**, *3*, 100157. DOI: 10.1016/j.nxmate.2024.100157.

[38] Zhang, D.; Luo, H.; Zheng, L.; Wang, K.; Li, H.; Wang, Y.; Feng, H. Utilization of Waste Phosphogypsum to Prepare Hydroxyapatite Nanoparticles and Its Application Towards Removal of Fluoride from Aqueous Solution. *J. Hazard. Mater.* **2012**, *241-242*, 418–426. DOI: 10.1016/j.jhazmat.2012.09.066.

[39] Nasrellah, H.; Yassine, I.; Hatimi, B.; Joudi, M.; Chemaa, A.; El Gaini, L.; Hatim, Z.; El Mhammedi, M. A.; Bakasse, M. New Synthesis of Hydroxyapatite from Local Phosphogypsum. *J. Mater. Environ. Sci.* **2017**, *8*, 3168–3174.

[40] Bensalah, H.; Bekheet, M. F.; Younssi, S. A.; Ouammou, M.; Gurlo, A. Hydrothermal Synthesis of Nanocrystalline Hydroxyapatite from Phosphogypsum Waste. *J. Environ. Chem. Eng.* **2018**, *6*, 1347–1352. DOI: 10.1016/j.jece.2018.01.052.

[41] *Handbook of Chemistry and Physics*, 95th ed.; CRC Press; Taylor & Francis Group: Boca Raton FL, **2014**.